Adsorption 5, 261–278 (1999)

Pressure Effects in Adsorption Systems

BHASKAR K. ARUMUGAM,* JEANNE F. BANKS,† AND PHILLIP C. WANKAT‡
School of Chemical Engineering, Purdue University, West Lafayette, IN 47907-1283, USA

Received March 13, 1998; Revised August 31, 1998; Accepted October 21, 1998

Abstract. A study of the occurrence of large pressure and flow transients when a strongly adsorbed gas is fed to a column which is initially loaded with a lightly adsorbed gas is presented here. Under certain conditions, these transients can cause premature breakthrough and change the shape of the breakthrough curve. This will result in improper estimation of adsorption parameters by the dynamic column loading method and lower apparent adsorption capacity in a full scale unit. A data acquisition system was used to record the pressure and flow transients. An isothermal PDE model developed to study these transients agreed reasonably well with the nonisothermal experimental results. The PDE model predicts that pressure and flow transients will occur during step and pulse tests conducted to obtain adsorption and mass transfer parameters by the chromatographic method. For instance, lower adsorption capacity will be realized during step tests due to lowering in column pressure. Oscillations were observed when columns are connected in series. The PDE model also predicts these oscillations. Simulations indicate that the extent of oscillations is dependent on the dead volume between columns.

Keywords: Adsorption, concentrated systems, pressure transients, flow transients

1. Introduction

Pressure Swing Adsorption (PSA) is a widely used technology for purification and bulk separation of gases. Various process improvements have been made since the early patents by Skarstrom (1960) and Guerin de Montgareuil and Domine (1964). Most theoretical studies of the PSA process have treated the adsorption and purge steps as isobaric. Recently, large pressure transients were observed in our lab when a strongly adsorbed gas (propane) was fed to a column filled with an inert gas (helium). Preliminary results (Arumugam and Wankat, 1996) will be briefly reviewed here to set the stage for the present work.

A column initially saturated with helium at an elevated pressure was fed with propane at the same pressure. The entering propane is strongly adsorbed while the nonadsorbed helium continues to flow out of the column resulting in a decrease in the total moles in the gas phase. The column pressure decreases, and since flow rates depend on pressure differences, the inlet flow rate increases while the outlet flow rate decreases. Clearly, the flow and pressure transients are a consequence of the continuity equation. Predictions from a single well-stirred tank model agreed qualitatively with experiments. A multiple tanks in series model predicted that pressure and flow oscillations occur which last until the feed breaks through. Oscillations occur in a staged system because as each stage is loaded with propane pressure first drops and then recovers as the adsorbent saturates. The pressure and flow oscillations are linked to the movement of the propane shock front. The model predictions agreed qualitatively with experiments conducted with three columns in series.

The simplicity of the stirred tank model facilitated the understanding of pressure transients. By staging tanks in series, the occurrence of oscillations in columns in series was discovered. Oscillations do not

*Present address. Eastman Chemical Company, Kingsport, TN.
†Present address. Amoco Fabrics and Fibers Co., Bainbridge, GA.
‡Author to whom correspondence is to be addressed.

occur in a single column which, as we will show, agrees with the solution of the PDE. However, the role of mass transfer resistance, which is expected to lower the magnitude of pressure and flow transients but enhance the duration, was ignored. Agreement between the staged model and packed column experiments requires fitting to determine the number of stages. A serendipitous advantage of the CSTR model was that it lead us to experimentally study columns in series where oscillations do occur. Thus, a partial differential equation model which includes mass transfer resistance was developed. Since manual recording of experimental pressure and flow data during the transient period was difficult, a fully automated data acquisition system was constructed to record the rapid transients more accurately.

2. Automated Data Acquisition System

The system is shown schematically in Fig. 1. A 100 cm stainless steel column with 5/8 in. internal diameter and 3/4 in. outer diameter was used. Taps were drilled on opposite sides of the column for pressure and temperature measurements. A square metal boss (side: 1.5 in., thickness: 0.75 in.) was welded to the column at each port to provide sufficient engagement between the tappings and probes. The first port was located at 6 cm from the inlet and the distance between adjacent ports was 22 cm. E type thermocouples were chosen since they have the highest sensitivity in the temperature range of interest. OMEGA PX181 pressure transducers with a 0–200 psig range and 1–5 Vdc output signal were used to measure column pressure. To prevent damage to pressure transducers from pressure shocks, a pressure snubber was fitted to the column at each port and the pressure transducer was connected to the pressure snubber.

The column was packed with 35–40 mesh Davison 5A molecular sieve between 4.8 cm from the inlet and 1.7 cm before the outlet; the empty space at the inlet and outlet ends was filled with glass wool. The column characteristics are given in Table 1. All simulations were initially conducted with $\rho_p = 1.534$ g/cm^3, but with this particle density, $\epsilon_e = 0.25$, which is low. Using a particle bulk density of 1.16 g/cm^3 (Table 6.1 in Ruthven (1984)), $\epsilon_e = 0.34$. When ϵ_e is changed, Darcy's law constants change considerably, but there is no significant change in simulation results. So, corrections were made only to those simulations where experiments are compared with theory. The value used in each simulation is indicated in figure captions.

A Matheson 8420, 0.4 to 20 SLM, mass flow controller with a maximum working pressure of 150 psi and a maximum pressure drop of 5 psi across the controller at maximum flow was used to measure inlet flow. The mass flow controller can be used as a mass flow meter if it is kept fully open.

All flow connections were made using 1/8 in. stainless steel tubing. A three-way solenoid valve with a maximum working pressure of 175 psi was used to

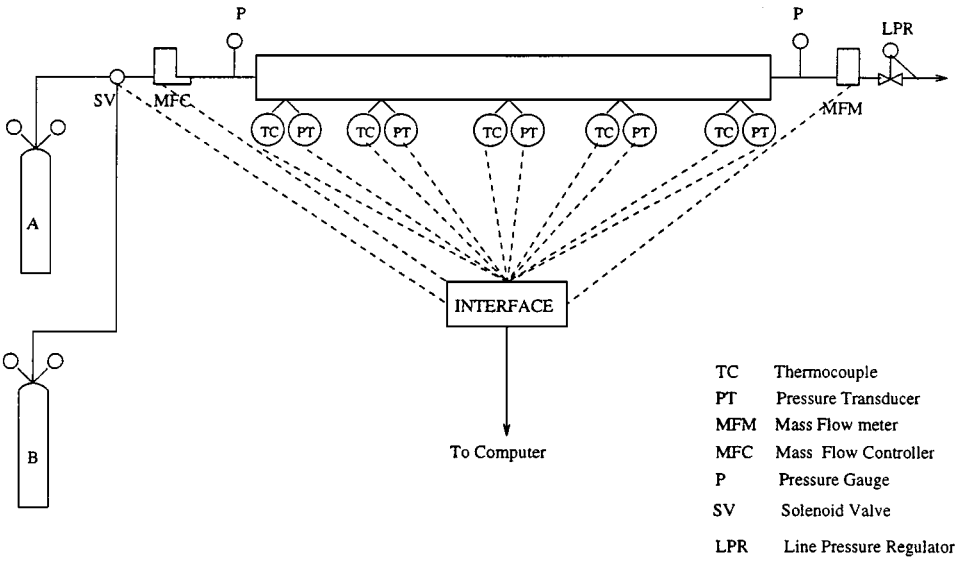

Figure 1. Schematic representation of data acquisition apparatus.

Table 1. Characteristics of adsorption columns used for automated data acquisition.

	Column 1	Column 2 (Section 7)
Internal diameter	5/8 in.	1/2 in.
External diameter	3/4 in.	3/4 in.
Column length	100 cm	25 cm
Port locations	6, 28, 50, 72, 94 cm	None
Packing length	93.5 cm	21.4 cm
Empty space at inlet end	4.8 cm	2.5 cm
Empty space at outlet end	1.7 cm	1.1 cm
Interparticle porosity	0.34	0.25
Intraparticle porosity (Table 6.1 in Ruthven, 1984)	0.34	0.34
Particle diameter	0.564 mm (35–40 mesh)	0.564 mm (35–40 mesh)
Macropore radius (Youngquist et al., 1971)	900 Å	900 Å
Particle bulk density (Table 6.1 on Ruthven, 1984)	1.16 g/cm^3	1.16 g/cm^3

switch inlet streams. The entire apparatus was located inside a hood for safety.

Analog signals from the five pressure transducers, five thermocouples, and mass flow controller were connected to a National Instruments interface board (NB-MIO-16X I/O connector). Digital signals from the interface board are acquired by Labview software installed on a Macintosh Quadra 700. Two analog outputs from the interface board are used to control the solenoid valve and the mass flow controller.

Numerous duplicate runs showed that flow, pressure, and temperature results were reproducible for both single columns and columns-in-series (Banks, 1996).

3. Model Development

The model was implemented within ADSIM (Aspen Technology, 1994) a flowsheeting environment from Aspen Technology, Inc. for the dynamic simulation of adsorption processes. The behavior of each unit is described by a model; units which are similar even if they differ in size and operating conditions are described by the same model. The flowsheet to study pressure transients has five units: feed, inlet valve, column, outlet valve, and sink. The inlet and outlet valve units are described by a common valve model; feed, column, and sink units have corresponding feed, column, and sink models.

3.1. Feed Model

The feed model simulates a constant pressure source with a given feed gas composition. The pressure, composition, and temperature of the feed gas are specified. Based on the source pressure of the feed unit and the column inlet pressure, the inlet valve determines the inlet flow rate. The molar flow rate of each species is then determined within the feed unit: $N_i = y_i N$. The feed model can be converted into a constant flow source model by specifying the feed flow rate instead of pressure. In that case, the inlet valve unit is removed from the flowsheet.

3.2. Valve Model

The valve model determines the molar flow rate based on the pressure on the inlet and outlet sides. The following equation was found to be satisfactory (Arumugam, 1996).

$$N = C_v \sqrt{P_{\text{in}}^2 - P_{\text{out}}^2} \tag{1}$$

Resistance to flow from connecting tubes, bends, etc., are included in C_v.

3.3. Bed Model

The column dynamics are described by material balances, steady state Darcy's law, mass transfer relations, and associated algebraic equations such as adsorption isotherms. The following assumptions were made in deriving the model: isothermal, linear driving force (LDF) approximation, Langmuir adsorption isotherm, axial pressure drop described by steady state Darcy's law, negligible axial and radial dispersion, and ideal gas mixture. The isothermality assumption is the most serious assumption in the model. In fact, experimental bed temperatures reached 80–90°C during the loading step (Banks, 1996). A rise in bed temperature caused by the heat of adsorption will reduce adsorption capacity. And, an increase in gas phase temperature will lead to an increase in pressure in accordance with the kinetic theory of gases. So, the simulations with a nonisothermal staged model showed smaller transients than for an isothermal system (Byrne, 1997).

The material balance is:

$$[\epsilon_e + (1-\epsilon_e)\epsilon_p]\frac{\partial C_i}{\partial t} + (1-\epsilon_e)(1-\epsilon_p) \times \rho_p \frac{\partial q_i}{\partial t} + \frac{\partial (vC_i)}{\partial z} = 0 \quad \text{where } i = A, B. \tag{2}$$

In various studies of pressurization and blowdown steps, the steady state Darcy or Ergun equation has been used, though these are transient steps. Sereno and Rodrigues (1993) investigated the validity of using steady state momentum balances to describe unsteady steps. They concluded that the steady state momentum equation is valid for modeling the pressure varying steps in a PSA cycle with non-porous, inert particles. Hart et al. (1990) in their study of pressure transients during pressurization and depressurization steps, found that the pressure dynamics can be explained using Darcy's law if a finite rate of adsorption is included. Darcy's law along with a fitted mass transfer coefficient was chosen to describe the pressure transients in this study.

$$\frac{dP}{dz} = \frac{150K_1\mu_g(1-\epsilon_e)^2}{D_p^2\epsilon_e^3}(\epsilon_e v) \tag{3}$$

where K_1 is a correction factor determined from steady state experiments.

The gas phase is assumed to be ideal,

$$C_i = \frac{y_i P}{R_g T} \tag{4}$$

Mass transfer to the solid is approximated by the linear driving force approximation based on the difference in the solid loading which would be in equilibrium with the gas phase and the solid loading,

$$\frac{dq_i}{dt} = k_{s,i}(q_s^* - q_s) \tag{5}$$

where $k_{s,i}$ is given by (Ruthven et al., 1994),

$$\begin{aligned} k_i &= \Omega_i \frac{\epsilon_p D_p}{R_p}\frac{c_o}{q_o} \quad \text{macropore control} \\ &= \Omega_i \frac{\epsilon_p D_c}{r_c^2} \quad \text{micropore control} \end{aligned} \tag{6}$$

and q^* is the equilibrium solid loading.

The solid loading in equilibrium with the gas phase, q_i^*, is related to the gas phase concentration by the multicomponent Langmuir isotherm:

$$q_i^* = \frac{K_i R_g T C_i}{\left(1 + \sum_{i=A,B} b_i R_g T C_i\right)} \tag{7}$$

Equation (7) is thermodynamically inconsistent unless all K_i/b_i are equal (LeVan and Vermeulen, 1981).

ADSIM can solve systems of coupled ordinary differential equations and algebraic equations. So, the partial differential equations have to be reduced to ordinary differential equations by discretizing the spatial derivative. A simple backward difference scheme was chosen to approximate the spatial derivatives.

The primary role of the sink model is to set the ambient pressure. The outlet flow rate is determined by the outlet valve unit based on the ambient pressure set in the sink unit and the column outlet pressure. The molar flow rate of each species is calculated within the sink model: $N_i = y_i N$.

4. Parameter Estimation

The validity of predictions of a model depends on the validity of the assumptions made in developing the model, the reliability of the parameters used in the model, and the solution procedure. The parameters occurring in the present model fall into the following categories: (1) column and adsorbent characteristics, (2) gas physical properties, (3) isotherm constants, (4) mass transfer coefficients, (5) Darcy's law constants, and (6) valve coefficients.

Physical characteristics of the column and adsorbent are given in Table 1. Viscosity (Liley et al., 1984) and molecular weights of the gases of interest are readily available. Literature values for Langmuir constants were used for ethane and propane (Youngquist et al., 1971) and an isotherm determined from experiment was used for methane (Arumugam, 1996) and helium is assumed to be nonadsorbed (Table 2).

Table 2. Isotherm constants (Arumugam, 1996 for methane and Youngquist et al., 1971 for ethane and propane) and gas viscosities (Liley et al., 1984.

Gas	K_i (mol/(kg atm))	b_i (atm^{-1})	μ (atm.s)
He	0.0	0.0	1.964×10^{-10}
CH_4	2.8385	1.0431	1.105×10^{-10}
C_2H_6	25.84	14.136	9.277×10^{-11}
C_3H_8	386.9	228	8.093×10^{-11}

4.1. *LDF Coefficients*

Calculations showed that diffusion in the macropores of the particle is in the transition regime between Knudsen and molecular diffusion at $P = 1$ atm (Arumugam, 1996). The molecular diffusivity of the binary gas mixture can be estimated from the Chapman-Enskog theory (Bird et al., 1960; Yang, 1987).

The relative importance of molecular and Knudsen diffusion is determined by the ratio of the pore diameter to the mean free path of the molecules (Yang, 1987). Molecular diffusion dominates if the ratio is greater than 10 and Knudsen diffusion dominates if the ratio is less than 0.1. The mean free path, λ, is $(\sqrt{2}\pi n\sigma^2)^{-1}$, where $n(=N_A P/R_g T)$ is the gas number density in molecules/volume and σ is the collision diameter. At 298.15 K, $n = 2.462 \times 10^{19} P$ (P in atm). The mean free path (cm) for helium, methane, ethane, and propane (Table 3) are in the range of the macropore diameter for Davison 5A molecular sieve (900 Å) at atmospheric pressure. The Knudsen diffusivities ($D_K = 2/3\bar{v}_A a$, where $\bar{v}_A = (8R_g T/\pi\ MW_A)^{1/2}$) are comparable to molecular diffusivities. Thus, diffusion under these operating conditions is intermediate between molecular and Knudsen diffusion.

The linear driving force mass transfer coefficient, $k_{s,i}$, is estimated from Eq. (6). The effective diffusivity in the Henry's law region is:

$$D_e = \frac{\epsilon_p D_p}{(1-\epsilon_p) b q_s} \tag{8}$$

where $D_p = \tau(1/D_k + 1/D_m)$ (Ruthven, 1984). For propane on Davison 5A (C-521) at 323 K (Ruthven, 1984), $\tau = 5.7$. The mass transfer coefficient for propane calculated from the Glueckauf approximation using literature isotherm constants (Youngquist et al., 1971) is low (0.009 s^{-1} at 2.361 atm). For ethylene in helium on zeolite 5A, Hassan et al. (1985) use a value of $k = 0.19\ s^{-1}$ at 3.0 atm. Estimates of the mass transfer coefficient using isotherm constants obtained from elution experiments are of the same order of magnitude as the value used by Hassan et al. (Table 4). Agreement between experiment and simulation results using these mass transfer coefficients was satisfactory.

Table 3. Knudsen and molecular diffusivities.

$R_g = 8.314 \times 10^7$ dyne cm/(mol K); $T = 298.15$ K

Gas	λ_i (cm)	$\bar{v}_i$ (cm/s)	$D_{K,i}$ (cm^2/s)	D_{AB} (cm^2/s)
He	$1.378 \times 10^{-5}/P$	1.256×10^5	0.3767	—
CH_4	$0.6259 \times 10^{-5}/P$	0.627×10^5	0.1882	$0.677/P$
C_2H_6	$0.4684 \times 10^{-5}/P$	0.458×10^5	0.1375	$0.5404/P$
C_3H_8	$0.3570 \times 10^{-5}/P$	0.378×10^5	0.1135	$0.4195/P$

Table 4. Darcy's law constant, K_1 and LDF coefficients, k_i. $\tau = 5.7$ was assumed for all species.

Gas	K_1 ($\epsilon_e = 0.25$)	K_1 ($\epsilon_e = 0.34$)	k_i s^{-1} (20 psig)	k_i s^{-1} (40 psig)
He	1.062	3.4485	—	—
CH_4	1.085	3.5238	1.818	1.480
C_2H_6	—	—	0.173	0.151
C_3H_8	1.188	3.8592	0.203	0.174

4.2. *Darcy's Law Flow Constant*

The correction factor, K_1 (Table 4), in Darcy's law was determined from a least squares fit of pressure drop and linear velocity data obtained from a limited set of experiments. The linear velocity was varied by changing the source pressure (Arumugam, 1996).

4.3. *Valve Coefficients*

The inlet valve coefficients for methane and propane were determined by independently fitting inlet flow rate and pressure drop across the inlet valve during the transient period (Arumugam, 1996). For helium, the inlet valve coefficient was calculated from steady state experiments using data on the flow and steady state pressure drop across the inlet valve. The outlet valve coefficient for all gases was determined from steady state experiments from flow and steady state pressure drop across the tubing, line pressure regulator, bends, etc., present on the outlet end. The valve coefficients are given in the figure captions.

5. Comparison of Experiments and Model Results

Simulations were started by pressurizing a column, initially filled with helium at 1 atm, from a helium source at either 2.32 or 3.72 atm. At $t = 50$ s, flow was switched to propane at the same source pressure. This is identical to the way experiments were conducted.

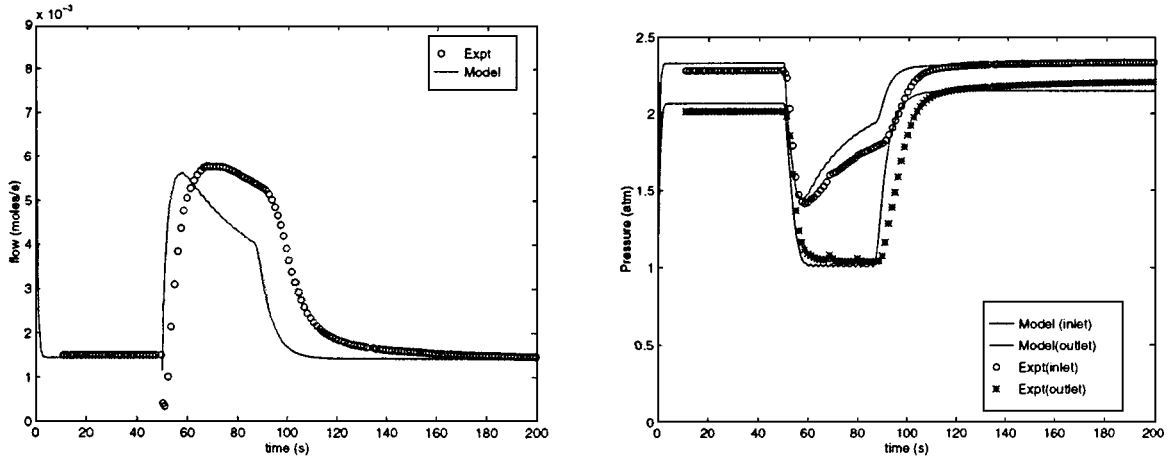

(a) Flow (b) Pressure

Figure 2. Comparison of experimental and model flow and pressure results when flow is switched from helium to propane ($P = 20$ psig, $\epsilon_e = 0.34$). Valve coefficients (mol/atm): $C_{\text{in}}(\text{helium}) = 3.8 \times 10^{-3}$, $C_{\text{out}}(\text{helium}) = 8.0 \times 10^{-4}$, $C_{\text{in}}(\text{propane}) = 3.0 \times 10^{-3}$, $C_{\text{out}}(\text{propane}) = 7.5 \times 10^{-4}$. Other simulation details given in Table 1–3. (a) Flow; (b) Pressure.

Oscillations observed in predicted curves for single columns are a numerical artifact; they can be reduced by increasing the number of finite difference nodes.

5.1. Switch from Pure Helium to Pure Propane at 2.32 atm

Comparisons of experimental flow and pressure results with model results are shown in Fig. 2. There is good agreement between experimental steady state helium flow and model predictions though there is a small offset between model and experimental inlet and outlet pressures. When flow is switched to propane (at $t = 50$ s), a rapid decrease in the inlet and outlet pressures was observed experimentally. Just after the switch, the inlet flow drops for a very short duration and then increases rapidly. The drop in experimental flow is probably caused by the valve. There is a drop in inlet flow rate in the model prediction too; the difference in valve coefficients for helium and propane is believed to cause this drop. The model results are in good agreement with experiments up to about 65 s though it predicts slightly faster changes than observed experimentally. This probably occurs because the model assumes instantaneous valve response. From 65–100 s, the agreement is not as good, but the general features are captured well. At steady state, following breakthrough, model predictions compare well with experiments. The duration of the transient period predicted by the model is shorter than the experiment. The agreement will be better if the saturation capacity predicted by the adsorption isotherm is increased. This can be inferred by comparing areas under the flow curves—the adsorbent has greater capacity for propane than predicted by the isotherm. A 10–15% variation in adsorption capacity between different lots of the same adsorbent is common (Ladisch, 1996); this variability could, to some extent, account for the mismatch between theory and experiment.

The experimental column temperature increased by more than 50°C (Fig. 3). Despite the large temperature excursion, the isothermal model predictions for flow and pressure match experimental results well during the initial period since the temperature wave is slow. During the later half of the transient period, the adsorbent temperature has increased resulting in greater discrepancy between model and experimental results. Assuming that the mass transfer coefficients do not vary with pressure and temperature probably contributes to the discrepancy too. An adiabatic staged model predicted a temperature maximum of 87°C (Byrne, 1997) which is in reasonable agreement with Fig. 3.

Internal pressures (Fig. 4) obtained from experiment compare well with model results particularly at short times. The behavior of internal pressures is intermediate of the inlet and outlet pressures.

Predicted axial concentration profiles (Fig. 5) show the movement of shock waves and the decrease in total concentration during the transient period. Due to the lower pressure, the column capacity is reduced

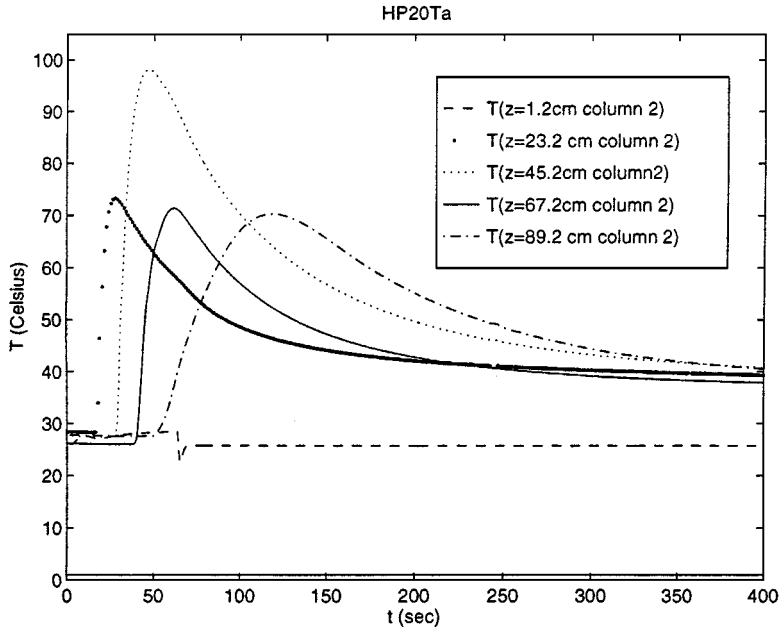

Figure 3. Temperature history when flow is switched from helium to propane ($P = 20$ psig, $\epsilon_e = 0.34$).

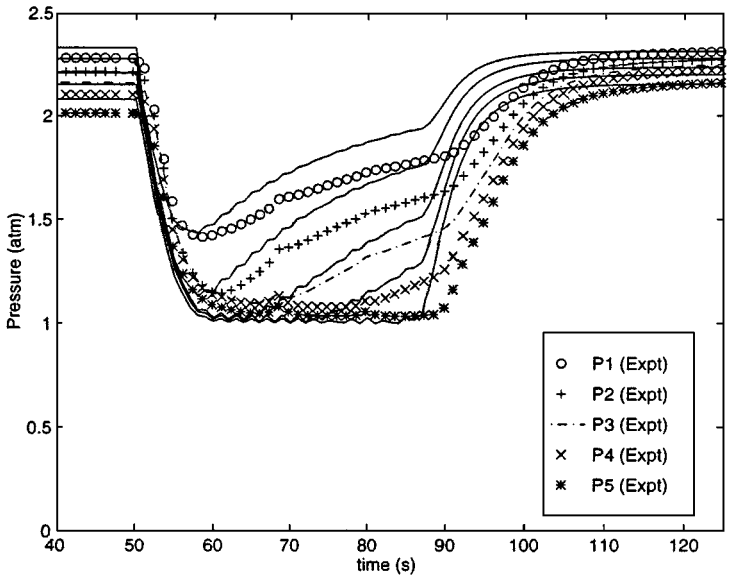

Figure 4. Comparison of experimental and model internal pressure results when flow is switched from helium to propane ($P = 20$ psig, $\epsilon_e = 0.34$). Simulation conditions given in Fig. 2.

resulting in earlier breakthrough. The discontinuity in the slope of concentration profiles is an artifact of using a limited number of nodes. If data is available at closer spacing across a shock transition, smoother curves will be obtained; however, with forty nodes the discontinuity in slopes persists. Similar discontinuities in the slope of concentration profiles appear in the literature (Finlayson, 1992).

It appears that the outlet concentration is more spread out than the outlet mole fraction curve (Fig. 6). When breakthrough occurs, the column is at a low pressure. The outlet concentration increases as the column

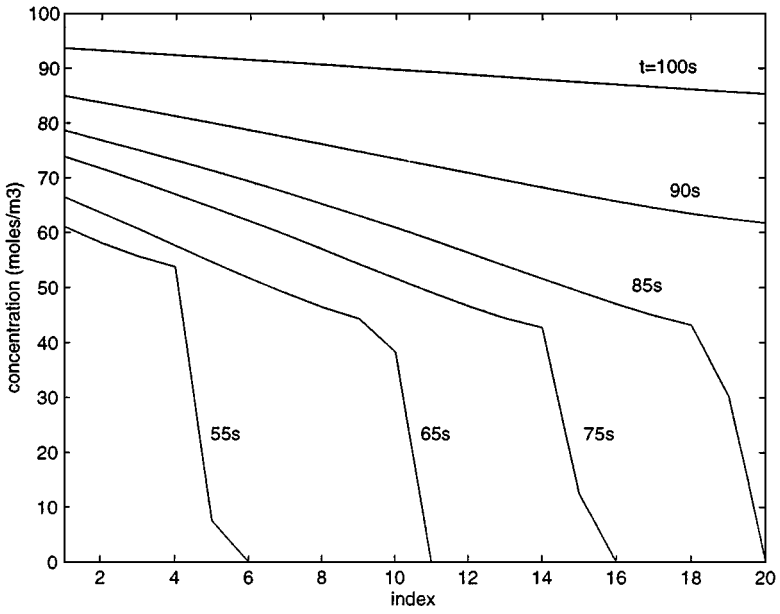

Figure 5. Predicted axial concentration profiles with twenty nodes showing movement of propane shock front when flow is switched from helium to propane ($P = 20$ psig, $\epsilon_e = 0.34$). Simulation conditions given in Fig. 2.

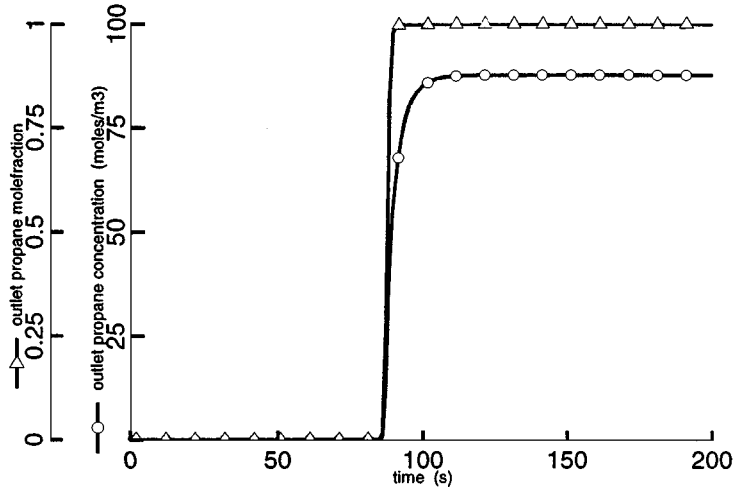

Figure 6. Simulation results showing breakthrough of propane shock front when flow is switched from helium to propane ($P = 20$ psig, $\epsilon_e = 0.34$). Simulation conditions given in Fig. 2.

pressure builds up following breakthrough; the outlet propane mole fraction becomes unity soon after breakthrough and is unaffected by subsequent increases in column pressure.

The ratio of the total moles of all species in the column at steady state after breakthrough to the total moles of all species in the column before feed is introduced serves as a convenient measure to determine the extent of pressure transients:

$$\chi = \frac{(1-\epsilon_e)(1-\epsilon_p)\rho_p V \Sigma q_{f,j} + [\epsilon_e + (1-\epsilon_e)\epsilon_p] V \Sigma C_{f,j}}{(1-\epsilon_e)(1-\epsilon_p)\rho_p V \Sigma q_{i,j} + [\epsilon_e + (1-\epsilon_e)\epsilon_p] V \Sigma C_{i,j}}. \tag{9}$$

For values of χ much greater than 1, pressure transients will be important. As χ decreases, approaching 1, the transients become less significant. For $\chi < 1$, pressure

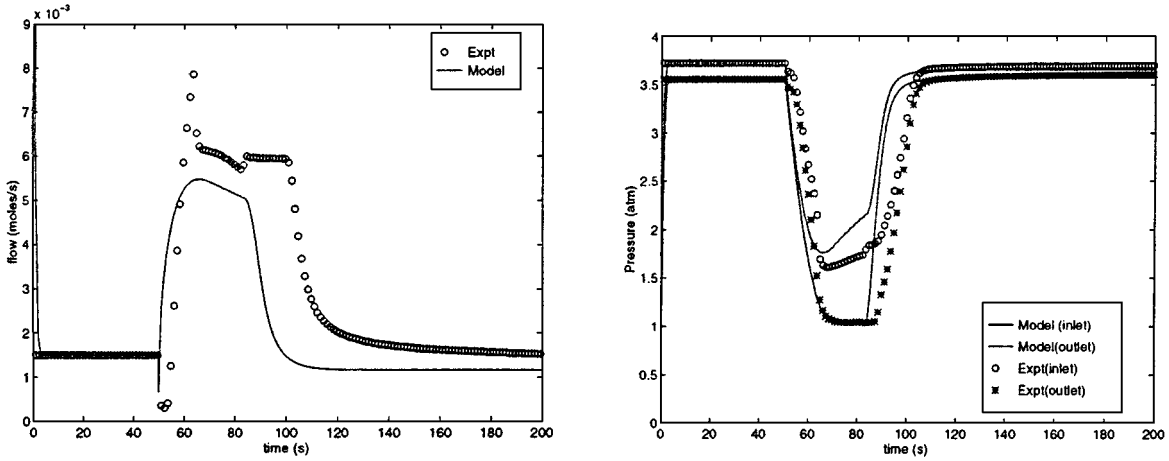

(a) Flow (b) Pressure

Figure 7. Comparison of experimental and model flow and pressure results for simulations where the flow is switched from pure helium to pure propane at 3.723 atm ($\epsilon_e = 0.34$). Valve coefficients (mol/atm): $C_{\text{in}}(\text{helium}) = 3.8 \times 10^{-3}$, $C_{\text{out}}(\text{helium}) = 8.0/1.8 \times 10^{-4}$, $C_{\text{in}}(\text{propane}) = 3.0/1.8 \times 10^{-3}$, $C_{\text{out}}(\text{propane}) = 7.5/2.2 \times 10^{-4}$. Other simulation details given in Tables 1–3. (a) Flow; (b) Pressure.

and flow transients of the type under consideration will not occur. When flow is switched from pure helium to pure propane at 20 psig, $\chi = 27.4$. As expected, large pressure and flow transients occur.

5.2. Switch from Helium to Propane at 3.723 atm

Comparison of experiment and model with source pressures at 3.723 atm reveals the same features. The valve coefficients in the model had to be changed to match inlet flow and inlet and outlet pressures at steady state (Fig. 7). The initial spike in inlet flow rate seen in experimental data was reproducible; its origin is not fully understood.

5.3. Switch from Helium to 52.5% Propane in Helium at $P = 2.32$ psig

A comparison of flow and pressure data from experiment and model where the feed is switched from pure helium to 52.5% propane in helium ($\chi = 26.89$) is shown in Fig. 8. The valve coefficients and Darcy's law constant for mixtures were assumed to be composition weighted averages of pure gas values. There is satisfactory agreement between the predicted and model pressure curves. The magnitude of pressure drop is lower than in Fig. 2(b) because 47.5% of the feed is helium which is not adsorbed. However, the duration of the transient period has almost doubled since the equilibrium adsorbent loading for 52.5% propane is very close to that for pure propane. The magnitudes of predicted and experimental flow transients do not agree, probably due to incorrect flow calibration.

6. Switch from Helium to Methane at 2.32 psig

Flow and pressure data from an experiment where the feed was switched from pure helium to pure methane is shown in Fig. 9. The transient period is much shorter in this case since the saturation capacity of the adsorbent for methane is lower than for propane. This is evident by comparing the areas under the flow curves for helium/methane (Fig. 9) with helium/propane (Fig. 2). This result supports the observation that differences in adsorption capacities of the initial gas and the feed gas cause pressure and flow transients. Additional experimental results where the feed is switched from pure methane to pure propane also support this observation (Banks, 1996).

7. Effect of Back Pressure Regulator

A back pressure regulator is often used in laboratories to maintain constant column pressure during loading studies. For small changes in concentration, the column pressure can be controlled satisfactorily. However, for a large change in feed concentration, the column pressure does vary significantly (Fig. 10). Note that the

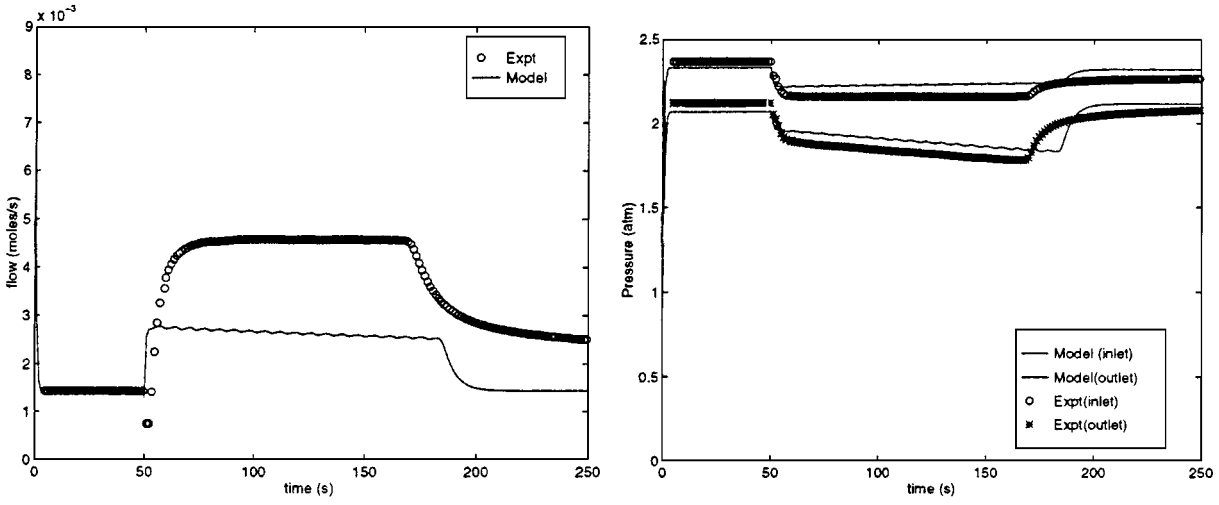

(a) Flow (b) Pressure

Figure 8. Comparison of experimental and model flow and pressure results from simulations where flow is switched from helium to 52.5% propane in helium at 2.36 atm ($\epsilon_e = 0.34$). Valve coefficients (mol/atm): 3. (a) Flow; (b) Presssure.

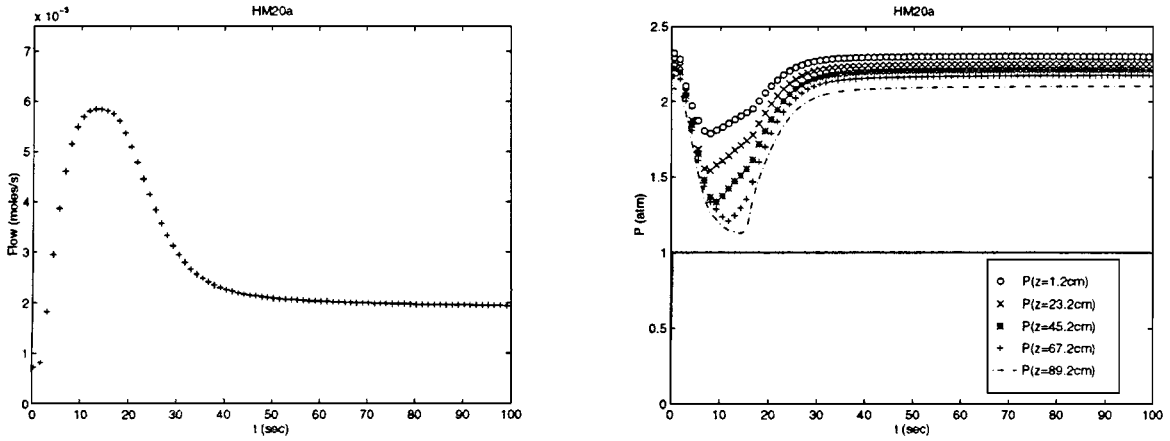

(a) Flow (b) Pressure

Figure 9. Experimental flow and pressure results where flow is switched from helium to methane at 2.36 atm (Table 1). (a) Flow; (b) Pressure.

magnitude of the transients is considerably lower in this case.

8. One-Column Simulations

8.1. Low Inlet Resistance

Simulations were conducted with the inlet valve coefficient ten times higher than the valve coefficient used previously. The major resistances to flow are friction in the bed and the outlet valve. The pressure drop between the source tank and the column inlet is low since the inlet resistance is low (Fig. 11). When feed is switched to propane from helium, strong adsorption causes a decrease in column pressure. But, since the inlet resistance is low, the inlet flow (Fig. 11, compare with Fig. 2) peaks at about twice the value with a lower valve coefficient. The adsorbent at the inlet end is swamped with propane because of the high inlet flow and hence the pressure drop at the inlet end (Fig. 11) is less drastic compared to Fig. 2. The outlet pressure drops to about the same value as in Fig. 2, but it reaches a steady value

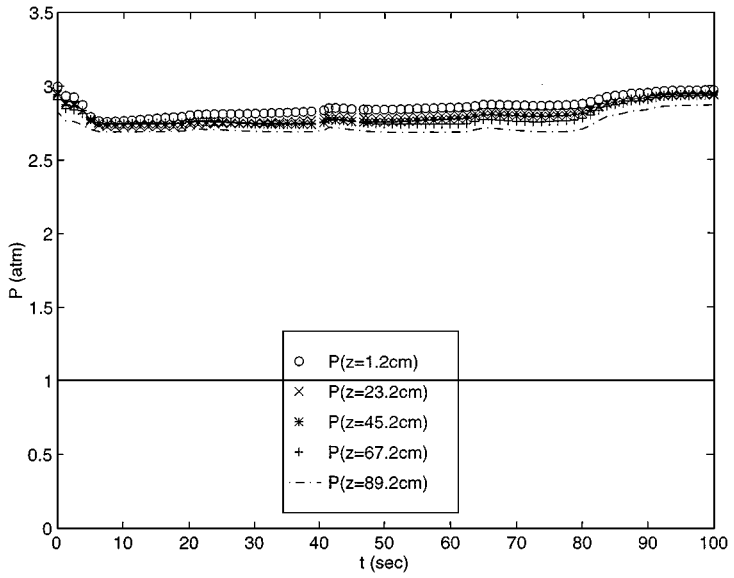

Figure 10. Total pressure profiles in column versus time. Column saturated with helium displaced by propane. Supply pressure = 30 psig.

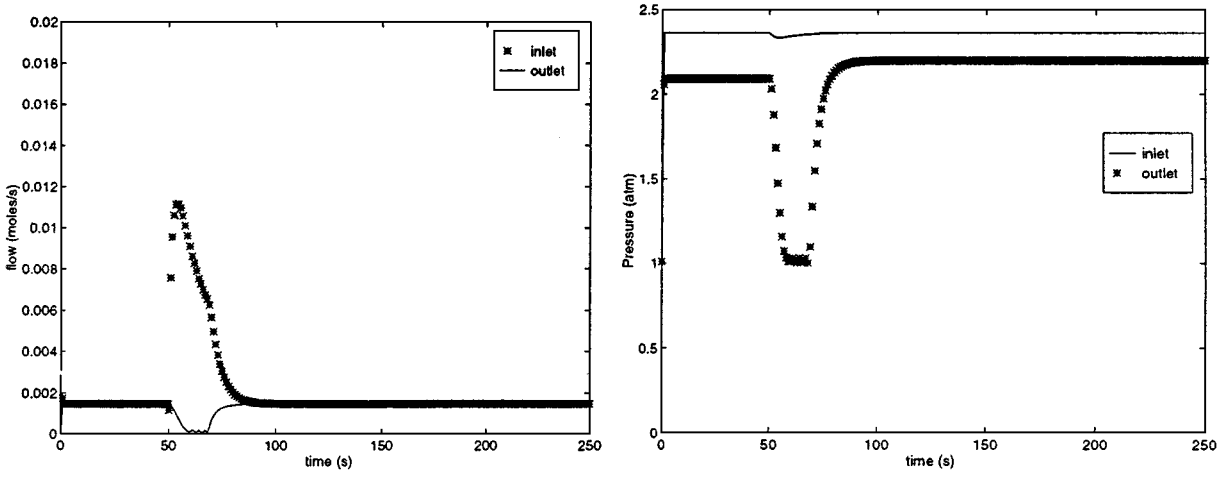

(a) Flow (b) Pressure

Figure 11. Predicted flow and pressure with low inlet valve resistance ($\epsilon_e = 0.25$). Valve coefficients (mol/atm): $C_{\text{in}}(\text{helium}) = 3.8 \times 10^{-3} \times 10$, $C_{\text{out}}(\text{helium}) = 8.0 \times 10^{-4}$, $C_{\text{in}}(\text{propane}) = 3.0 \times 10^{-3} \times 10$, $C_{\text{out}}(\text{propane}) = 7.5 \times 10^{-4}$. Other simulation details given in Tables 1–3. (a) Flow; (b) Pressure.

earlier. Due to the larger flow, breakthrough occurs sooner and the duration of transients is shorter.

8.2. Constant Inlet Flowrate

The increased inlet flow rate during the transient period acts as a feedback mechanism that attempts to minimize the pressure transients. If the inlet flow rate is held constant, the transients will last longer since the feedback mechanism is removed. Figure 12 shows flow and pressure predictions with the inlet flow rate held constant at 1.44×10^{-3} mol/s. As expected the transient period lasts longer and breakthrough occurs later (Arumugam, 1996).

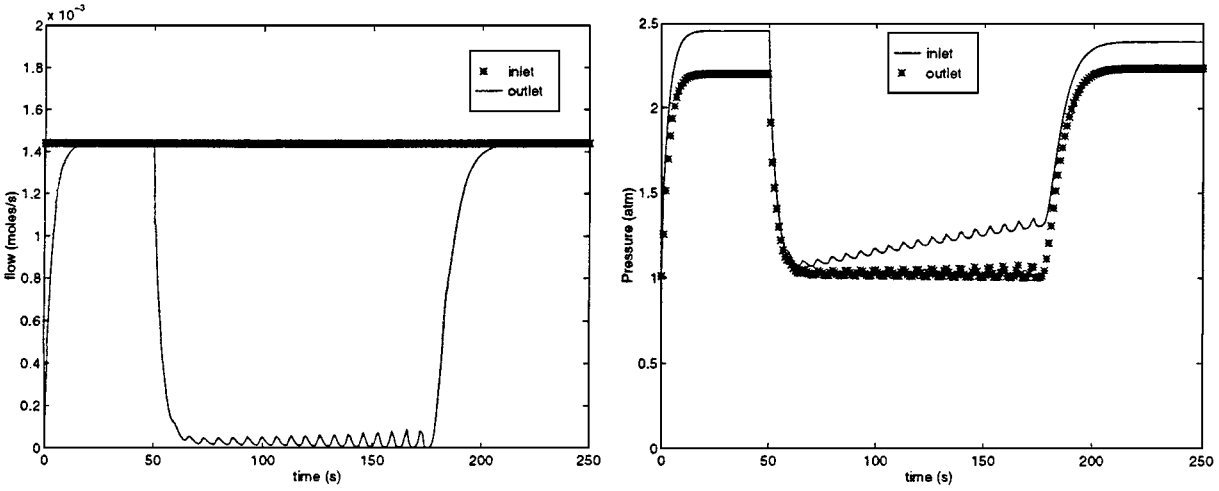

(a) Flow (b) Pressure

Figure 12. Predicted flow and pressure for simulations with constant inlet flow rate (1.44×10^{-3} mol/s, $\epsilon_e = 0.25$). Valve coefficients (mol/atm): $C_{\text{out}}(\text{helium}) = 8.0 \times 10^{-4}$, $C_{\text{out}}(\text{propane}) = 7.5 \times 10^{-4}$. Other simulation details given in Tables 1–3. (a) Flow; (b) Pressure.

An overall material balance assuming that the column pressure remains constant shows that the mean breakthrough time is:

$$\tau = \frac{\text{increase in solid loading} + \text{increase in amount in gas phase}}{\text{inlet flow rate}}$$

$$= \frac{(1-\epsilon_e)(1-\epsilon_p)\rho_p V(q_f - q_i) + [\epsilon_e + (1-\epsilon_e)\epsilon_p]V(c_f - c_i)}{yN_{\text{in}}} \tag{10}$$

For this example, $\tau = 171.5$ s. Since the switch occurs at 50 s, mean breakthrough should occur at $\tau = 221.5$ s if the column pressure remained constant. But, since the column pressure is lower, breakthrough occurs sooner, at approximately 180 s. Thus, the decrease in column pressure results in a loss of adsorption capacity.

8.3. Low Mass Transfer Coefficient

The adsorbent responds slower when flow is switched from helium to propane if the mass transfer coefficient is lower. Thus, the column pressure does not drop the same extent (Fig. 13, compare with Fig. 2), and consequently, the magnitude of the rise in inlet flow rate is less (Fig. 13). So, though χ is a useful parameter in determining the extent of transients, other factors can modify system behavior. Breakthrough occurs sooner since mass transfer is poor (Fig. 14), but, since it takes longer to saturate the column, the transients last longer.

8.4. Step and Pulse Inputs

Chromatographic methods are frequently employed to determine effective diffusivities from breakthrough curves. In these studies, axial pressure drop is generally neglected (Gibilaro and Waldram, 1972; Kawazoe et al., 1974; Kumar et al., 1982; Raghavan et al., 1985) though the system has been analyzed with axial pressure drop included (Chiang et al., 1984; Dixon et al., 1988; KershenBaum and Kohler, 1984; Pazdernik and Schneider, 1981). Irrespective, pressure is assumed to be invariant with time. Simulations conducted to examine the validity of the assumption that the column pressure is invariant with time during step and pulse experiments are presented in this section.

To a column saturated with 5% propane in helium, a feed consisting of 10% propane in helium is introduced (at $t = 500$ s) with the inlet flow rate held constant at 1.44×10^{-3} mol/s. There is a small decrease in column pressure (Fig. 15) which lasts until breakthrough occurs at about 560 s (Fig. 16). This is accompanied by a decrease in the outlet flow rate (Fig. 15).

A 10 s pulse of 10% propane is introduced into a column initially saturated with 5% propane (switch time = 500 s). Again, there is a small decrease in column pressure, both at the inlet and the outlet ends, and the outlet flow rate. Breakthrough occurs at approximately 560 s (Arumugam, 1996).

Large step changes are employed in industry to determine adsorption capacity and mass transfer parameters.

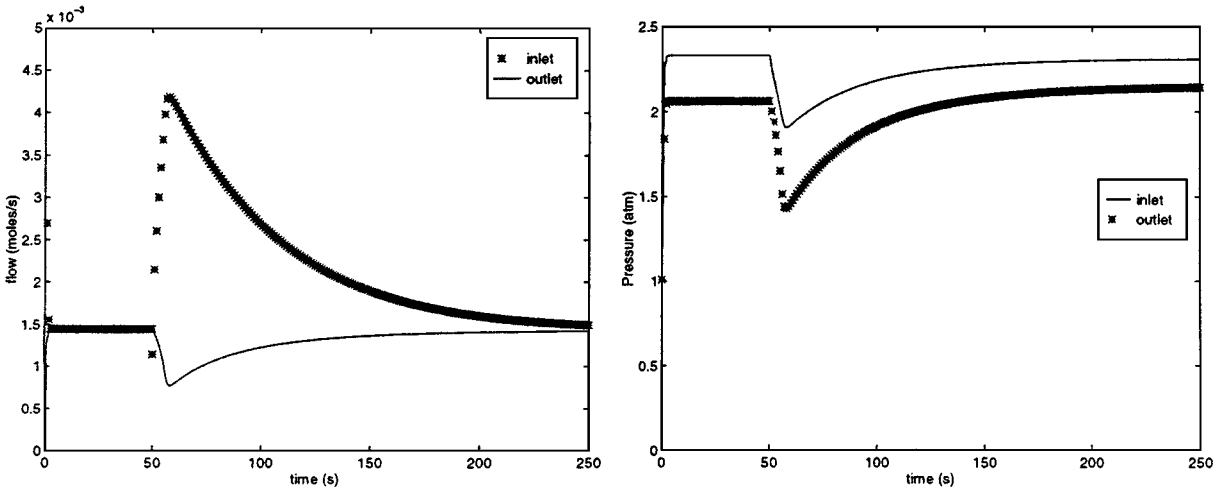

(a) Flow (b) Pressure

Figure 13. Predicted flow and pressure with low mass transfer coefficient ($\epsilon_e = 0.25$). Valve coefficients (mol/atm): $C_{\text{in}}(\text{helium}) = 3.8 \times 10^{-3}$, $C_{\text{out}}(\text{helium}) = 8.0 \times 10^{-4}$, $C_{\text{in}}(\text{propane}) = 3.0 \times 10^{-3}$, $C_{\text{out}}(\text{propane}) = 7.5 \times 10^{-4}$; $k_{\text{propane}} = 0.0174$ 1/s. Other simulation details given in Tables 1–3. (a) Flow; (b) Pressure.

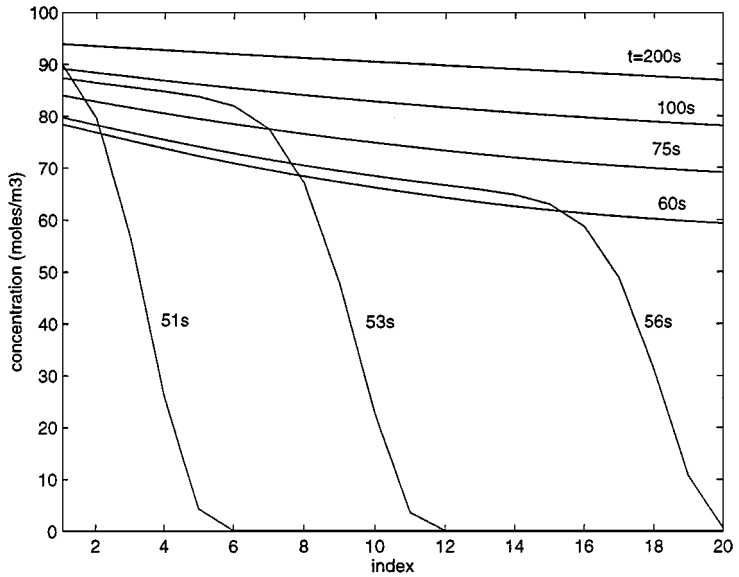

Figure 14. Axial concentration profiles for simulations with low mass transfer coefficient ($\epsilon_e = 0.25$). Simulation conditions given in Fig. 13.

For example, to determine mass transfer parameters for air separation, a step input of air is fed to a column containing oxygen (Note: This is a much larger step than used in these simulations). A constant inlet flow rate is maintained in these experiments. The above simulation results suggest that pressure changes are likely to occur during such step experiments. The pressure changes can be a source of error in the estimation of adsorption and mass transfer parameters. Appropriate instrumentation to control the column pressure such as a back pressure regulator (Section 7) will minimize the pressure transient. However, under certian conditions, the pressure transient can still be significant. Malek and Farooq (1996) present a mathematical

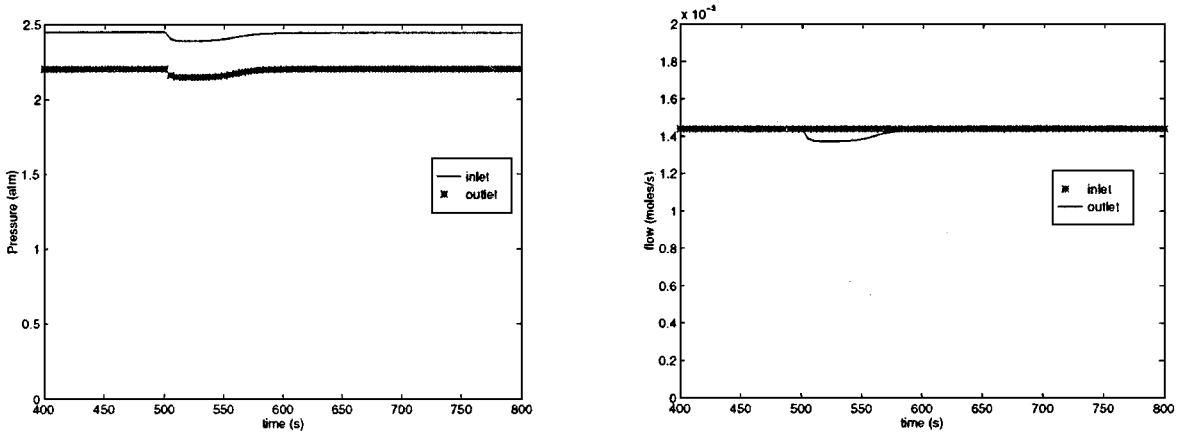

(a) Pressure (b) Flow

Figure 15. Simulation pressure results for a step input ($\epsilon_e = 0.25, 1.44 \times 10^{-3}$ m/s). Valve coefficients (mol/atm): $C_{\text{out}}(\text{helium}) = 8.0 \times 10^{-4}$, $C_{\text{out}}(\text{propane}) = 7.5 \times 10^{-4}$. Other simulation details given in Tables 1–3. (a) Pressure; (b) Flow.

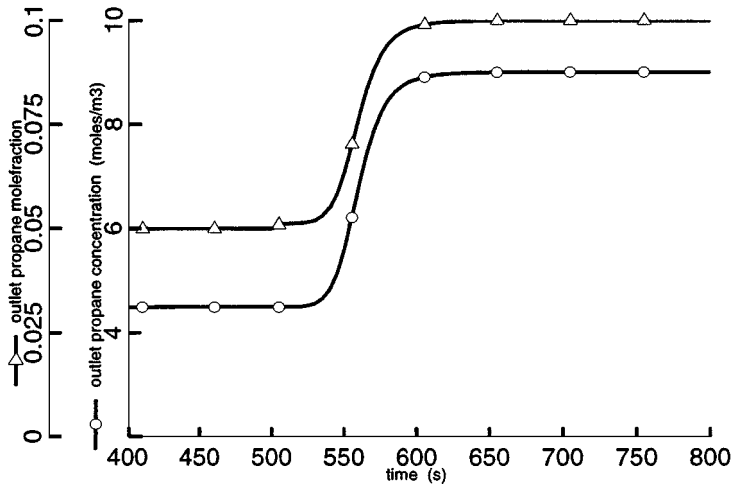

Figure 16. Outlet concentration and mole fraction for simulations where a small step is input to the column ($\epsilon_e = 0.25$). Simulation conditions given in Fig. 15.

framework to accomodate the effect of pressure changes.

9. Columns-in-Series

For columns-in-series, the tube connecting adjacent columns is a unit and requires a model describing it. By setting $\epsilon_e = 1$ in Eq. (2), the material balance for an empty tube is obtained.

$$\frac{\partial C_i}{\partial t} + \frac{\partial (vC_i)}{\partial t} = 0 \tag{11}$$

The flow through the connecting tubes is assumed to be described by the differential form of the Hagen-Poiseuille equation (Bird et al., 1960),

$$C \frac{D^2}{64 R_g T \mu_g} \frac{dP}{dz} = v. \tag{12}$$

This equation is valid for laminar flow under steady state in tubes; here it is used as a relation to describe flow in the tube with C as a fitting factor which will account for flow expansion and contraction at the tube ends.

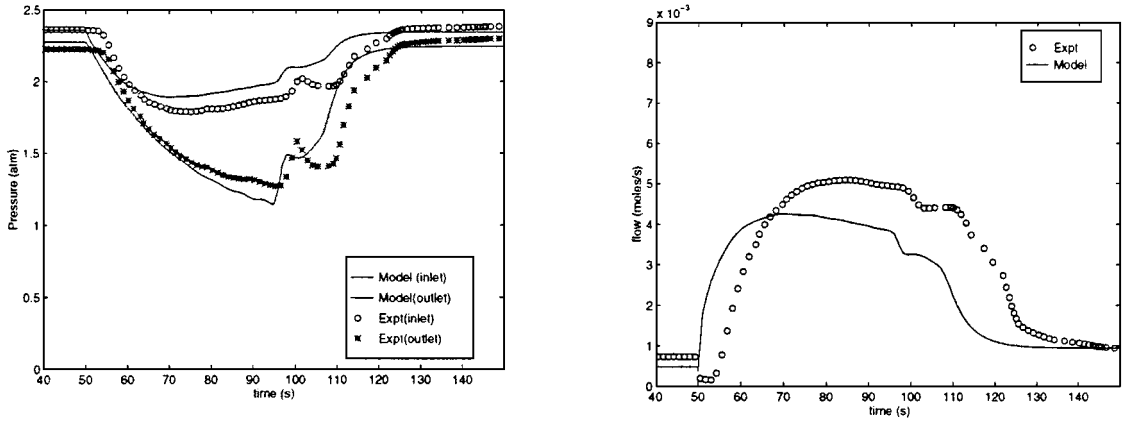

(a) Pressure (b) Flow

Figure 17. Comparison of pressures at inlet and outlet of column 1 and of inlet flow rate of column 1 for two columns in series ($\epsilon_{e,1} = 0.34$, $\epsilon_{e,2} = 0.25$). Valve coefficients (mol/atm): $C_{\text{in}}(\text{helium}) = 3.8 \times 10^{-3}$, $C_{\text{in}}(\text{propane}) = 3.0 \times 10^{-3}$. Outlet tube constants: $D = 0.175 \times 10^{-2}$ m, length = 0.40 m, $C = 5 \times 10^{-5}$. Connecting tube: $D = 0.875 \times 10^{-6}$ m^3, length $= 9 \times 10^{-2}$ m, $C = 4.44 \times 10^{-4}$. Other simulation details given in Tables 1–3. (a) Pressure; (b) Flow.

A second bed, described by the same bed model, was connected to the existing bed with a connecting tube. The outlet of the second bed was connected to the sink by a outlet tube instead of the valve. Unlike the connecting tube, the outlet tube is assumed to have no volume. The constant in Darcy's law for column 2 is assumed to be the same as for column 1. Since the occurrence of oscillations was the main interest in solving the columns-in-series model, forty nodes per column were used to minimize numerical oscillations.

In the experimental apparatus, a second column (Table 1) was connected to the outlet of the first column. Instead of a line pressure regulator, a needle valve was connected at the outlet of the second column.

Comparison of experimental and model inlet and outlet pressures and inlet flow rate are shown in Fig. 17. Both model and experiments show reproducible oscillations in pressures and flow (Arumugam, 1996; Banks, 1996). As expected from the results of the staged model (Arumugam and Wankat, 1996), the occurrence of oscillations is linked to the movement of the shock wave. When flow is switched from helium to propane, the pressure in both columns starts decreasing because of adsorption occurring in column 1. When breakthrough occurs from column 1 to column 2 (Fig. 18), the pressure in both columns starts increasing and the inlet flow starts decreasing. But, when the shock wave reaches the inlet of the second column, adsorption in the second column causes a decrease in pressure in both columns and an increase in inlet flow. The extent of oscillations depends on the time taken by the shock wave to traverse the dead volume between the two columns. In the experiment, the dead volume at the outlet of the first column is 3.25×10^{-6} m^3; at the inlet of the second column, 3.17×10^{-6} m^3; and in the connecting tube, 0.22×10^{-6} m^3 (total dead volume is 6.66×10^{-6} m^3). In the model, the connecting tube alone introduces dead volume ($D = 0.875 \times 10^{-2}$ m, length $= 9 \times 10^{-2}$ m, volume $= 6.55 \times 10^{-6}$ m^3). At steady state, the molar flow rate is approximately, 7.0×10^{-4} mol/s (volumetric flow rate: 7.26×10^{-6} m^3/s). At this flow rate, the time constant of the dead volume is 0.9 s. The effective time constant will be higher since the outlet flow rate from column 1 is lower than the steady state value until the shock wave exits column 1.

The pressure at the inlet and outlet of the second column was not measured. Simulation results of the pressures and flows at the inlet and outlet of both columns are shown in Fig. 19. There is insignificant pressure drop across the connecting tube since the tube diameter is large. When the dead volume in the connecting tube is reduced by a factor of ten (volume $= 6.55 \times 10^{-7}$ m^3), the extent of oscillations reduces (Arumugam, 1996).

If three columns are connected in series, up to three pressure minima are observed (Arumugam, 1996). When the location of the two columns was switched so that the short column was first, the bump in pressure and flow rate occurred much earlier as expected (Banks, 1996).

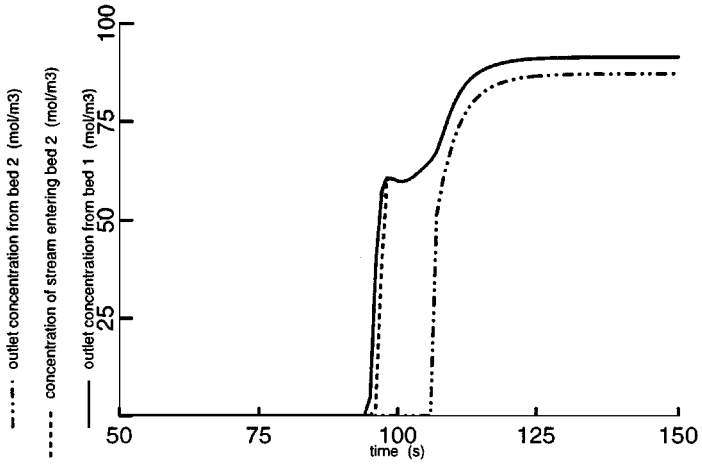

Figure 18. Simulation results: Breakthrough curves for two columns in series ($\epsilon_{e,1} = 0.34$, $\epsilon_{e,2} = 0.25$). Simulation conditions given in Fig. 17.

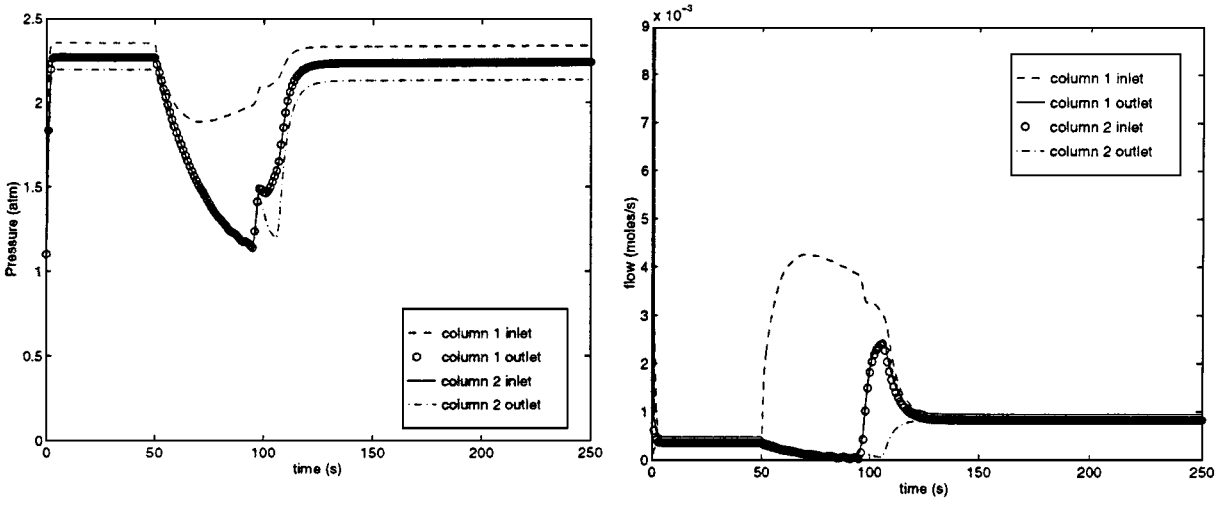

(a) Pressure (b) Flow

Figure 19. Simulation results: Pressure and flow rates at inlet and outlet of columns 1 and 2 ($\epsilon_{e,1} = 0.34$, $\epsilon_{e,2} = 0.25$). Simulation conditions given in Fig. 17. (a) Pressure; (b) Flow.

10. Discussion and Conclusions

The present model captures the general features of the transient pressure behavior of an adsorption column satisfactorily. An elaborate non-isothermal model which considers macropore diffusion, surface diffusion, and intracrystalline diffusion would describe the system more accurately. But, determining the parameters involved in the model is difficult. The LDF approximation with a fitted mass transfer coefficient is usually satisfactory for equilibrium selectivity based separations.

The mass transfer coefficient, presently estimated from molecular diffusivity, Knudsen diffusivity, and experimentally determined isotherm constants, should be determined by comparing model and experimental outlet concentrations. Since breakthrough occurs quickly, nearly continuous breakthrough curves could not be obtained experimentally. Other gas mixtures containing gases like oxygen or carbon dioxide for

which continuous concentration analyzers are available should be studied. In addition, pressure dependence of the mass transfer coefficients should be considered.

Simulations of step and pulse runs have shown that pressure transients do occur during these experiments unless corrective counter measures are taken. The extent to which these transients affect measurements of adsorption capacity and mass transfer coefficients should be investigated.

The dimensionless parameter, χ, provides an a priori estimate, based on equilibrium capacities, of the extent of pressure transients. The transients are important if $\chi \gg 1$. However, other factors such as mass transfer resistances modify the nature of these transients. Since the column pressure is lowered, adsorption capacity is lowered and hence breakthrough occurs earlier. Also, the concentration breakthrough curve is more spread out than the mole fraction curve.

Oscillations occur when columns are connected in series. The extent of oscillations depends on the time constants of the dead volumes between columns. In industry, columns are connected in series for various reasons such as to incorporate pressure equalization steps and to limit the size of individual beds. Adsorption columns are often packed with layers of different adsorbents. Depending on the differences in adsorptivities of feed components in the layers, such columns can possibly exhibit oscillations, particularly if there are big differences in adsorption capacities of adjacent layers.

Nomenclature

b	constant in Langmuir isotherm	atm^{-1}
c, C	gas phase concentration in bulk flow	mol/cm^3
C_v	flow coefficient for valves and regulators	—
d_p	particle diameter	cm
D	1. tube diameter	m
	2. diffusivity	cm^2/s
k	mass transfer coefficient	s^{-1}
K	1. constant in Darcy's law	
	2. constant in Langmuir isotherm	mol/g atm
N	molar flowrate	mol/s
P	pressure	atm
q	solid phase loading	mol/g
R_g	gas constant	atm/(gmol K)
t	time	s
T	absolute temperature	K
v	linear interstitial gas velocity	cm/s
V	bed volume	cm^3
z	axial distance in bed	cm

Greek Letters

ϵ_e	interstitial void fraction	—
ϵ_p	intraparticle void fraction	—
τ	1. defined by Eq. (10)	—
	2. tortuosity	
Ω	cycle time dependent constant in Eq. (6)	—
μ	viscosity of gas phase	g/cm s
ρ_p	particle density	g/cm^3
χ	defined by Eq. (9)	—

Superscripts

$*$	equilibrium
T	total

Subscripts

i	component i
in	inlet conditions
j	component j
out	outlet conditions
o	reference conditions
s	saturation

Acknowledgment

This research was partially supported by NSF grant CTS-9401935.

References

ADSIM User Manual, Aspen Technology, Cambridge, Massachusetts, USA, 1994.

Arumugam, B.K., "Bulk Multicomponent Adsorption and Pressure Transients in Adsorption Systems," Ph.D. Thesis, Purdue University, West Lafayette, IN, 1996.

Arumugam, B.K. and P.C. Wankat, "Pressure Behavior During the Loading of Adsorption Systems," *Fundamentals of Adsorption*, M.D. LeVan (Ed.), pp. 51–58, Kluwer Academic Publishers, Massachusetts, 1996.

Banks, J., "Pressure Behavior During the Loading of Gas Adsorption Systems," Master's Thesis, Purdue University, 1996.

Bird, R.B., W. Stewart, and E.N. Lightfoot, *Transport Phenomena*, p. 150, John Wiley and Sons, 1960.

Byrne, M., "Pressure Effects in Adiabatic Adsorption and Adsorptive Reactors," Master's Thesis, Purdue University, 1997.

Chiang, A.S., A.G. Dixon, and Y.H. Ma, "The Determination of Zeolite Crystal Diffusivity by Gas Chromatography—I. Theoretical," *Chemical Engineering Science*, **39**(10), 1451–1459 (1984).

Dixon, A.G. and Y.H. Ma, "A Comparison of Moment Methods for Non-Isobaric Gas Chromatography Columns," *Chemical Engineering Science*, **43**(6), 1297–1302 (1988).

Finlayson, B.A., *Numerical Methods for Problems with Moving Fronts*, Ravenna Park Publishing, Seattle, Washington, 1992.

Gibilaro, L.G. and S.P. Waldram, "The Evaluation of System Moments from Step and Ramp Response Experiments," *Chemical Engineering Journal*, **4**, 197–198 (1972).

Guerin de Montgareuil, P. and D. Domine, U.S. Patent no. 3,155,468, 1964.

Hart, J., M.J. Battrum, and W.J. Thomas, "Axial Pressure Gradients During the Pressurization and Depressurization Steps of a PSA Gas Separation Cycle," *Gas Separation and Purification*, **4**, 97–102 (1990).

Hassan, M., N.S. Raghavan, D.M. Ruthven, and H.A. Boniface, "Pressure Swing Adsorption. Part II. Experimental Study of a Nonlinear Trace Component Isothermal System," *AIChE Journal*, **31**(12), 2008–2025 (1985).

Kawazoe, K., M. Suzuki, and K. Chihara, "Chromatographic Study of Diffusion in Molecular-Sieving Carbon," *Journal of Chemical Engineering of Japan*, **7**(3), 151–157 (1974).

KershenBaum, L.S. and M.A. Kohler, "Adsorption in Non-Isobaric Fixed Beds—II. Measurements of Rates of Adsorption," *Chemical Engineering Science*, **39**(9), 1423–1426 (1984).

Kumar, R., R.C. Duncan, and D.M. Ruthven, "A Chromatographic Study of Diffusion of Single Components and Binary Mixtures of Gases in 4A and 5A Zeolites," *Canadian Journal of Chemical Engineering*, **60**, 493–499 (1982).

Ladisch, M., *Personal Discussions*, 1996.

LeVan, M.D. and T. Vermeulen, "Binary Langmuir and Freundlich Isotherms for Ideal Adsorbed Solutions," *J. Phys. Chem.*, **85**(22), 3247–3250 (1981).

Liley, P.E., R.C. Reid, and E. Buck, "Physical and Chemical Data," Table 3–309, *Perry's Chemical Engineers' Handbook*, 6th edition, McGraw-Hill, NY, 1984.

Malek, A. and A. Farooq, "Determination of Equilibrium Isotherms Using Dynamic Column Breakthrough and Constant Flow Equilibrium Desorption," *J. Chem. Eng. Data*, **41**, 25–32 (1996).

Pazdernik, O. and P. Schneider, "Peak Moments for Gas Chromatographic Columns with a Pressure Drop," *Journal of Chromatography*, **207**, 181–191, (1981).

Raghavan, N.S. and D.M. Ruthven, "Simulation of Chromatographic Response in Columns Packed with Bidisperse Structured Particles," *Chemical Engineering Science*, **40**(5), 699–706 (1985).

Ruthven, D.M., *Principles of Adsorption and Adsorption Processes*, John Wiley and Sons, New York, 1984.

Ruthven, D.M., S. Farooq, and K.S. Knaebel, *Pressure Swing Adsorption*, VCH Publishers, New York, NY, USA, 1994.

Sereno, C. and A. Rodrigues, "Can Steady-State Momentum Equations be Used in Modelling Pressurization of Adsorption Beds?," *Gas Separation and Purification*, **7**(3), 167–174 (1993).

Skarstrom, C.W., U.S. Patent no. 2,944,627, 1960.

Yang, R.T., *Gas Separation by Adsorption Processes*, Butterworth Publishers, Stoneham, MA, USA, 1987.

Youngquist, G.R., J.L. Allen, and J. Eisenberg, "Adsorption of Hydrocarbons by Synthetic Zeolites," *Industrial and Engineering Chemistry: Product Research and Development*, **10**(3), 308–314 (1971).